Freezing between Two and Three Dimensions

Matthias Schmidt and Hartmut Löwen*

Institut für Theoretische Physik II, Heinrich-Heine-Universität Düsseldorf, Universitätsstrasse 1, 40225, Düsseldorf, Germany

(Received 26 February 1996)

The freezing transition of hard spheres confined between two parallel hard plates is studied for different plate separations interpolating between two and three spatial dimensions. Using Monte Carlo simulations and free volume theory, the full phase diagram is obtained exhibiting solid-to-solid transitions between buckled, layered, and rhombic crystals. While the fluid-solid transition is always strongly first order, both strong and very weak transitions occur between different crystalline structures. All predicted transitions should be experimentally observable in confined colloids. [S0031-9007(96)00444-9]

PACS numbers: 64.70.Dv, 61.20.Ja

The physics of fluids confined between two parallel plates can be quite different from their three-dimensional (3D) bulk behavior as the confinement drastically affects structural correlations, dynamical properties [1], and the location of phase transitions [2]. The dimensionality of the confined fluid may be continuously interpolated between three and two by varying the plate separation distance from macroscopic towards molecular spacings. Many recent studies devoted to the freezing transition in strictly three- or two-dimensional fluids have demonstrated that the transition can be quite different in 3D and 2D [3]. While it is a first-order transition in 3D, it may be a two-stage continuous transition in 2D with an intermediate hexatic phase possessing long-ranged bond-orientational order.

Much less is known about freezing of fluids limited in one direction, i.e., systems intermediate between 2D and 3D. In recent years, this subject has received a boost from experiments on colloidal dispersions confined between two glass plates [4–6]. Such samples are realizations of confined fluids on a mesoscopic length scale with the advantage that the particle trajectories can be followed directly by video microscopy and correlations can be measured in real space. For varying plate separations, a sequence of crystalline layerings were observed corresponding to a cascade of solid-solid transitions. Theoretical work, on the other hand, is much less comprehensive and has mainly been done in the framework of a hard-sphere model confined between hard walls: Pieranski and co-workers have calculated the close-packed density [7] and used a cell model to calculate some solid-to-solid transitions [8]. The structure of the confined hard sphere fluid was investigated by Percus [9] and Wertheim, Blum, and Bratko [10], but without addressing the freezing transition. Finally, within a Landau approach, a transition from a crystalline monolayer to a buckled solid phase was recently pointed out by Chou and Nelson [11].

The aim of this Letter is to determine by Monte Carlo (MC) simulation the full phase diagram for the confined hard-sphere model for arbitrary density and plate separations lying between one and two sphere diameters. The phase diagram is found to exhibit a rich structure with a fluid phase and many different solid phases including buckled, layered, and rhombic crystalline structures. We find a first-order freezing transition which can be followed by a further solid-to-solid transition as the density is increased. Interestingly enough, these solid-to-solid transformations can be strong or very weak. We also present a simple theory for the phase diagram, combining free volume theory of the crystalline phase with an effective-diameter theory of the fluid phase, which yields qualitative and semiquantitative agreement with our exact simulation data.

Our model consists of N hard spheres of diameter σ confined between parallel hard plates with area A and gap thickness $H = (h + 1)\sigma$, such that $h = 0$ corresponds to the 2D limit of hard disks. Since temperature is irrelevant for excluded-volume interactions, the only thermodynamic quantities are the reduced particle density $\rho_H = N\sigma^3/AH$ and the effective reduced plate separation h. The particle coordinate perpendicular to the plates is z, with $-h\sigma/2 \leq z \leq h\sigma/2$.

In our Monte Carlo simulations, we use the canonical ensemble with particle numbers ranging from $N = 192$ to $N = 1156$ in order to check systematically for finite-size effects. Careful attention is paid to the boundary conditions, which are crucial in a system exhibiting structural phase transitions. To allow any periodically ordered structure to fit into the simulation box for a suitable particle number N, the box is allowed to change its shape in the course of the simulation while its volume is fixed. The area in the lateral plane is a parallelogram with periodic boundary conditions. MC moves concerning its angles and aspect ratio are performed, so that the system can relax to equilibrium via shearing and squeezing. Between 10 and 100×10^6 MC steps per particle were computed to determine the equation of state for fixed h in the region of a phase transition. Phase transitions are detected by looking for van der Waals loops in the equation of state for fixed h. By performing a Maxwell

 0031-9007/96/76(24)/4552(4)$10.00

construction, the corresponding density jump is calculated by equating both the lateral pressures $p_{\mathrm{lat}} = -H^{-1}dF/dA$ (F denoting the Helmholtz free energy) and the chemical potentials of the coexisting phases. As a consistency check, we have also used the single occupancy cell method [12] for $h = 0.85$ finding the same phase boundaries. In addition, we have monitored the behavior of suitably defined order parameters in order to characterize the emerging crystalline phases. We introduce a set of double-indexed complex order parameters Ψ_{mn}, defined via $\Psi_{mn} \equiv \langle N^{-1} \sum_{\alpha=1}^{N} |\Psi_n(\alpha)| \exp[im \arg \Psi_n(\alpha)] \rangle$. Here $\langle \cdots \rangle$ denotes a canonical average and $\Psi_n(\alpha) \equiv N_\alpha^{-1} \sum_\beta \exp(in\Theta_{\alpha\beta})$, where the sum is over N_α neighbors of particle α possessing lateral distances smaller than 1.2σ and having opposite signs in their z coordinates and $\Theta_{\alpha\beta}$ is the angle between the bond of particles α and β and an arbitrary axis. The quantity Ψ_{mn} tests for solid structures with an $(m \cdot n)$-fold rotational symmetry. By calculating the order parameter set $\{\Psi_{mn}\}$ during the simulation, one can readily distinguish between different local surroundings of particles and thus identify the crystalline structure. An abrupt change in the order parameters signals a phase transition.

In Fig. 1 the resulting phase diagram is shown in the plane spanned by the reduced particle density ρ_H and the effective plate spacing h. The region in phase space is naturally limited by the close-packed density (dashed line). Different symbols represent different system sizes showing that the dependence on system size is only weak. For $h = 0$, in agreement with recent simulations of Weber and co-workers [13], we recover the first-order freezing transition of hard disks into a triangular lattice. As h is increased, the fluid freezes first into one triangular layer and with increasing density subsequently undergoes a further first-order transition into a crystalline structure of buckled lines (b). For intermediate h, the fluid freezes into two layers of a square lattice ($2\square$) via a strong first-order transition and then transforms into the buckling phases (b). The latter transition is marked by $\triangle$ symbols indicating phase boundaries, where the equation of state shows no van der Waals loop, but the order parameters exhibit anomalous behavior. Within the finite resolution of the simulation we could not distinguish whether such a transition is weakly first order or continuous. However, for $h = 0.6$, for example, we can exclude a density jump $\Delta\rho_H$ larger than 0.0004. Hence the $2\square \rightarrow b$ transition is extremely weak. For even higher h, a transition occurs from the $2\square$ phase into a crystal with two triangular layers ($2\triangle$). Finally there is a new stable crystalline phase which we call rhombic (r) since its unit cell is a rhombus. It is a close-packed structure but its stability also extends towards slightly smaller densities. The $2\square \rightarrow r$ and $2\triangle \rightarrow r$ transitions are again very weak.

Let us add some more details for the two less common phases b and r. Typical particle configurations and

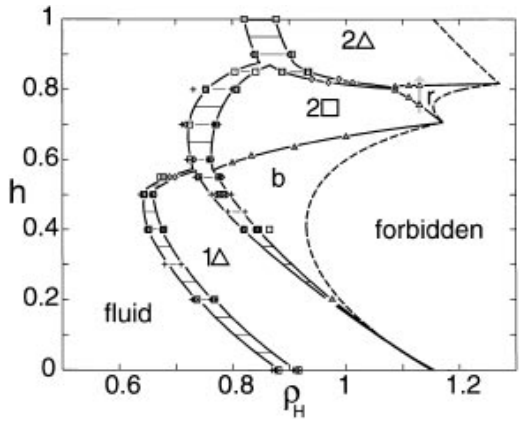

FIG. 1. Simulated phase diagram for hard spheres of reduced density ρ_H between parallel plates with effective reduced separation h. Symbols indicate different system sizes: $N = 192$ (+); $N = 384, 512$ (◇); $N = 576$ (△); $N = 1024, 1156$ (□). The statistical error is of the order of the symbol size. Six phases occur (fluid, $1\triangle$, b, $2\square$, r, and $2\triangle$). The closed-packed density is marked by a dashed line. Solid lines are guides to the eye. Thin horizontal "tie-lines" represent two-phase coexistence.

the corresponding unit cells are depicted in Figs. 2(a) and 2(b). Both structures possess two-fold rotational symmetry. Interestingly enough both the buckling and the rhombic phase are *highly degenerate*. For the buckling phase, there is linear buckling (constituted by a single rectangular unit cell), periodic zig-zag buckling (built up from left and right kites), and a random succession of both [shown in Fig. 2(a)]. Still, in the horizontal direction, there is strict periodicity. Likewise, the rhombic phase can appear to be linear rhombic (with a single rhombic elementary cell), zig-zag rhombic (with an alternating succession of the two rhombi), and again a random succession of both as shown in Fig. 2(b). All of these structures are close packed at the corresponding values of h. Away from close packing we cannot distinguish within our simulation which of these phases is the thermodynamically stable one since the free energy differences are too miniscule. Let us remark that this is quite similar to the 3D hard-sphere crystal, where the three close-packed structures fcc, hcp, and random stacking are extremely close in free energy and the actual crystalline structure depends on the history of the sample.

The identification of the different solid phases is illustrated in Fig. 3 where the behavior of three order parameters Ψ_{14}, Ψ_{21}, and Ψ_{23} is shown across the $2\square \rightarrow r$ and $r \rightarrow 2\triangle$ transition (see the grey arrow in Fig. 1). In the region where the $2\square$ structure is stable, the quantity Ψ_{14} reaches its maximum value while Ψ_{23} vanishes. On the other hand, Ψ_{14} vanishes in the $2\triangle$ region when Ψ_{23} is almost unity. The intermediate region is not a two-phase-coexistence region: As can be deduced from a nonvanishing Ψ_{21}, a structure with a two-fold rotational

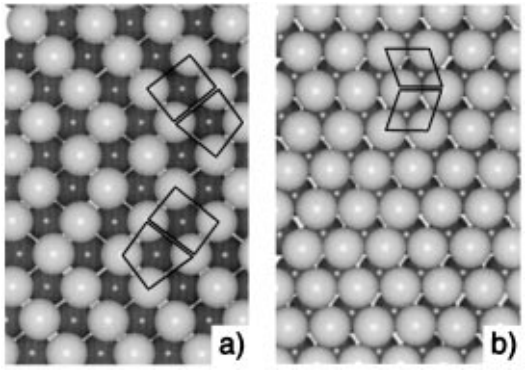

FIG. 2. Typical configurations of the *b* and *r* phases. Note the strict periodicity in the horizontal direction. (a) *Buckling phase.*—The four different local neighborhoods are marked as two "kites" and two rectangles with different relative orientations. (b) *Rhombic phase.*—Two differently oriented rhombi are shown.

symmetry is stable, which is further identified with the rhombic phase by inspecting typical configurations.

We emphasize that the fluid freezing transition is first order. In fact we checked that bond-angle orientational correlation functions with two, four, and sixfold symmetry decay exponentially with distance in the fluid phase and reach a finite plateau value in the solid phase. At least for a system size of $N \leq 1156$, we never found an intermediate "duatic," "tetratic," or "hexatic" phase characterized by an algebraic decay of the corresponding orientational correlation. This fact, of course, does not exclude the occurrence of such phases in larger systems and in systems that are governed by softer interactions.

Let us now briefly describe our theoretical approach. The solid phases are described using the cell model proposed in Ref. [8], which has an explicit solution in the 3D bulk [14]. The free volume cell is a shrunken Wigner-Seitz cell of the underlying fcc lattice with a lattice constant $(a - \sigma)/2$, a denoting the nearest-neighbor distance in the fcc lattice. For confined hard spheres, however, the free volume cell changes also its shape as the density is varied. This implies that the number of free lattice parameters is larger than the number of constraints, in contrast to 3D where only the parameter a is fixed by prescribing the density. Maximizing the free volume V_f numerically with respect to the additional parameters, the final value of $-k_BT\ln(V_f/\sigma^3)$ provides an upper bound for the free energy per particle, k_BT denoting the thermal energy.

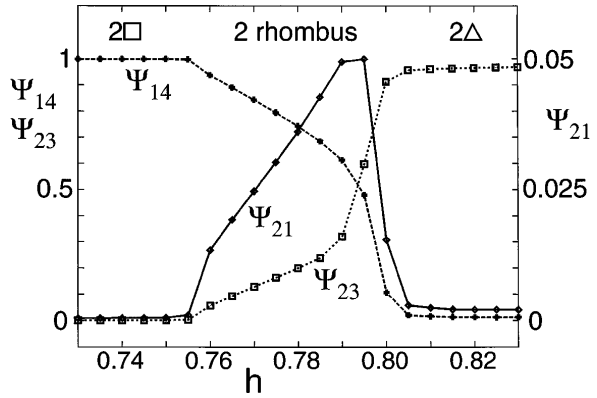

FIG. 3. Behavior of the order parameters Ψ_{14}, Ψ_{21}, and Ψ_{23} in three different phases (2□, *r*, and 2△) versus h for $\rho_H = 1.134$. This path is indicated in Fig. 1 as a grey arrow.

The fluid in slab geometry is approximately treated as a strictly two-dimensional hard-disk system with an effective diameter σ^* obtained from the implicit relation

$$(\sigma^*)^2 = \sigma^2 - \int_{-h\sigma/2}^{h\sigma/2} dz_1 \int_{-h\sigma/2}^{h\sigma/2} dz_2 \times (z_1 - z_2)^2 \rho(z_1, \sigma^*) \times \rho(z_2, \sigma^*)/[\rho_H(h+1)\sigma^{-2}]^2, \quad (1)$$

where the one-particle density profile $\rho(z, \sigma^*)$ is given by $\rho_H(h+1)\exp[\alpha(\sigma^*)z^2]/\mathcal{N}(\alpha(\sigma^*))$ with normalization $\mathcal{N}(\alpha) = \sqrt{\pi/\alpha}\,\sigma^2 \mathrm{erfi}(\sqrt{\alpha}\,h\sigma/2)$ and $\alpha(\sigma^*) = \pi\rho_H(h+1)g(\sigma^*)/\sigma^2$, erfi denoting the imaginary error function. Here, $g(\sigma^*) = [1 - \eta(\sigma^*)/2]/[1 - \eta(\sigma^*)]^2$ is the contact value of the 2D pair correlation function within scaled particle theroy, and $\eta(\sigma^*) = (\pi/4)\rho_H(h+1)\sigma^{*2}/\sigma^2$ is the effective area fraction of the 2D system. The expression (1) takes into account the fact that two spheres can be laterally closer than σ if they differ in their z coordinates. Finally the Helmholtz free energy is obtained via integration of $dF/dA = -k_BT\rho_H(1+h)[1 + \pi\rho_H(h+1)\sigma^{*2}g(\sigma^*)/2\sigma^2]/\sigma^2$ guaranteeing the correct second virial coefficient in the low density limit. The integration constant F_0 is empirically chosen to fit the location of the hard-disk freezing transition.

The theoretical phase diagram is shown in Fig. 4. It looks similar to the exact simulation data reproducing the stability of the six different phases found in the simulation [15]. All transitions are first order. The density gap between $b \rightarrow 2\square$ and $r \rightarrow 2\triangle$ is extremely small in agreement with the simulation; for instance, $\triangle\rho_H = 0.00047$ at $h = 0.72$ for the $b \rightarrow 2\square$ transition. Also the fluid $\rightarrow 1\triangle$ and $1\triangle \rightarrow b$ transitions are quantitatively correct. Another interesting property concerns the above-mentioned degeneracy of the *b* and *r* phases. Indeed, also away from close packing, the free volumes are identical for different realizations of the *b* and *r* phases and hence the cell model cannot distinguish between the subspecies. One can thus conclude that the cell model, which requires much less numerical effort than a direct simulation, gives reliable results as far as the topology of the phase diagram of confined hard-body systems is concerned. Some details of the phase diagram, however, are not reproduced. The slope of the $2\square \rightarrow b$ line is positive in simulation but negative in cell theory. Hence the cell theory overestimates

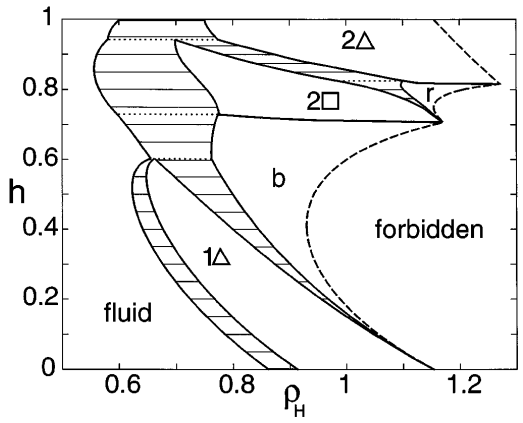

FIG. 4. Same as Fig. 1 but now obtained from effective-diameter and cell theory. The dotted tie lines represent regions with three coexisting phases [19].

the stability of the buckled phase. Furthermore, the agreement of the fluid-solid coexistence region grows worse as h increases since within effective-diameter theory we map a multilayer fluid onto a single-layer fluid.

In conclusion, we have calculated the phase diagram of hard spheres confined between two parallel hard plates for small plate separations H ranging from one to two sphere diameters. We have not considered possible transition structures from two to three layers, which emerge at $H > 1.82\sigma$ for high densities. In that case, even more crystalline structures can compete in free energy and the phase diagram becomes increasingly complicated. Our work is complementary to Ref. [16] working in the grand-isostress ensemble and to Ref. [17] focusing on transitions in a multilayer system.

We finish with a couple of remarks: First, although solely excluded volume interactions enter in our model, it may be used also for softer interactions as long as they can be mapped onto an effective hard sphere system confined between effective hard plates. In particular, a charged suspension between charged plates could be treated in this manner if the salt content is high. Second, an experimental verification of the full phase diagram is highly desirable in confined sterically-stabilized colloidal suspensions or in charged but highly salted dispersions. Using video microscopy or scattering methods one should be able to locate the various transitions in order to test our predictions. We finally mention that similar solid-solid transitions were recently found [18] for bilayer Wigner crystals in a double quantum-well system exposed to a strong magnetic field.

We thank H. Wagner, Y. Rosenfeld, A. Hüller, P. Leiderer, T. Palberg, S. Neser, and A. Denton for helpful discussions. This work was supported by the Deutsche Forshcungsgemeinschaft within the Gerhard-Hess-Programm.

*Also at Institut für Festkörperforschung, Forschungszentrum Jülich, D-52425 Jülich, Germany.

[1] *Molecular Dynamics in Restricted Geometries*, edited by J. Klafter and J. M. Drake (John Wiley, New York, 1989).
[2] P. A. Thompson, G. S. Grest, and M. O. Robbins, Phys. Rev. Lett. **68**, 3448 (1992).
[3] K. J. Strandburg, Rev. Mod. Phys. **60**, 161 (1988).
[4] P. Pieranski, L. Strzelecki, and B. Pansu, Phys. Rev. Lett. **50**, 900 (1983).
[5] D. H. Van Winkle and C. A. Murray, Phys. Rev. A **34**, 562 (1986); C. A. Murray, W. O. Sprenger, and R. A. Wenk, Phys. Rev. B **42**, 688 (1990); C. A. Murray, in *Bond-orientational Order in Condensed Matter Systems*, edited by K. J. Strandburg (Springer, New York, 1992).
[6] J. Weiss, D. W. Oxtoby, D. G. Grier, and C. A. Murray, J. Chem. Phys. **103**, 1180 (1995).
[7] B. Pansu, P. Pieranski, and P. Pieranski, J. Phys. (Paris) **45**, 331 (1984).
[8] A. Bonissent, P. Pieranski, and P. Pieranski, Philos. Mag. A **50**, 57 (1984).
[9] J. K. Percus, J. Stat. Phys. **23**, 657 (1980).
[10] M. S. Wertheim, L. Blum, and D. Bratko, in *Micellar Solutions and Microemulsions: Structure, Dynamics, and Statistical Thermodynamics*, edited by S.-H. Chen and R. Rajagopalan (Springer, New York, 1990).
[11] T. Chou and D. R. Nelson, Phys. Rev. E **48**, 4611 (1993).
[12] W. G. Hoover and F. H. Ree, J. Chem. Phys. **47**, 4837 (1967); see also D. Frenkel and A. J. C. Ladd, J. Chem. Phys. **81**, 3188 (1984).
[13] H. Weber and D. Marx, Europhys. Lett. **27**, 593 (1994); H. Weber, D. Marx, and K. Binder, Phys. Rev. B **51**, 14 636 (1995).
[14] J. G. Kirkwood, J. Chem. Phys. **18**, 380 (1950).
[15] A modification of cell theory is done for the 1△ phase where we inserted a different effective diameter $\sigma^*_{1\triangle} = \sigma\sqrt{1 - h^2/6}$ into the expression for the 1△-free volume in order to enlarge the free volume for two touching spheres with different z coordinates.
[16] D. J. Diestler, M. Schoen, and J. H. Cushman, Science **262**, 545 (1993).
[17] J. E. Hug, F. van Swol, and C. F. Zukoski, Langmuir **11**, 111 (1995).
[18] L. Zheng and H. A. Fertig, Phys. Rev. B **52**, 12 282 (1995); S. Narasimhan and T.-L. Ho, Phys. Rev. B **52**, 12 291 (1995).
[19] Note that the Gibbs phase rule, which admits a maximum of two coexisting phases in the 2D and 3D bulk case, is not violated here due to the additional freedom of the transversal pressure $-A^{-1}dF/dH$.